ROMANIAN JOURNAL OF INFORMATION SCIENCE AND TECHNOLOGY
Volume **12**, Number 2, 2009, 249–263

Spotted cDNA microarray image segmentation using ACWE

Shenghua NI[1], Pan WANG[2], Mihaela PĂUN[3,2], Weizhong DAI[2], Andrei PĂUN[4,5,1]

[1] Department of Computer Science/IfM, Louisiana Tech University, P.O. Box 10348, Ruston, LA 71272, USA,

E-mail: {shn004,apaun}@latech.edu

[2] Department of Mathematics and Statistics, Louisiana Tech University, P.O. Box 10348, Ruston, LA 71272, USA,

E-mail: {pwa003, mpaun, dai}@latech.edu

[3] Faculty of Mathematics and Informatics, Spiru Haret University, Bucharest, Romania,

[4] Bioinformatics Department, National Institute of R&D for Biological Sciences, Splaiul Independenţei, Nr. 296, Sector 6, Bucharest, Romania,

E-mail: apaun@dbio.ro

[5] Universidad Politécnica de Madrid - UPM, Facultad de Informática Campus de Montegancedo S/N, Boadilla del Monte, 28660 Madrid, Spain,

E-mail: andrei.paun@upm.es

Abstract. The segmentation of the picture (and, implicitly, the segmentation method used) is one of the three important steps in microarray image processing, together with spot gridding and information extraction. It directly affects the accuracy of gene expression analysis in the data mining process that follows. In 2001 a segmentation method for arbitrary pictures using the Active Contours Without Edges (ACWE) technique to detect the objects boundaries was proposed. In this paper we present a segmentation method based on ACWE with applications in cDNA segmenting. Because of the targeted nature of the method proposed we were able to perform several adjustments to the original method and use it in the cDNA microarray image processing area. We present various experiment results showing that the ACWE method is better than the

other segmentation methods used in the cDNA microarray and that the results obtained match more closely (than the older methods) the biological cycle through correct gene expression measurements.

1. Introduction

A DNA microarray is an array of DNA spots. One type of DNA microarray is called complementary DNA (cDNA) microarray. In cDNA microarrays DNA strands are fastened at fixed spots on glass or plastic slides or silicon chips. A cDNA microarray is a useful tool for analyzing gene expression based on the samples of genes in the spots aligned in a regular pattern. cDNA microarrays provide widely used technology for doing scientific experiments simultaneously with thousands of genes or entire genomes. This approach is much more efficient than the traditional experiment method which only focuses on a few genes at one time. A critical part in the gene analysis process is the effectiveness of image segmentation analysis. There are four types of segmentation methods described in [8]: fixed circle segmentation, adaptive circle segmentation, adaptive shape segmentation and histogram segmentation. Some cDNA microarrays segmentation software have been developed based on the four types segmentation methods. ScanAlyze developed by Eisen in 1999 is based on the fixed circle segmentation method. This method assumes that the spot has a perfect circle shape and all spots have the same size. GenePix developed by Axon Instruments Inc. in 1999 uses, on the other hand, an adaptive circle segmentation method. This method assumes as well that the spot has a circular shape but also allows for adjusting the size of each spot. It provides more accurate results than the fixed circle method. SpotSegmentation is a software based on histogram segmentation [5], and was developed by Qunhua Li and Chris Fraley in 2005. The method uses a clustering algorithm to partition the pixels based on their pixels intensity values. Most of the histogram segmentation algorithms neglect the spatial information of pixels. SpotSegmentation is the modified method which combined the power of the histogram-based and spatial approaches. SPOT is a software developed by Y.H. Yang, M. J. Buckley and T. P. Speed in 2002 and described in [8]. and applied the adaptive shape segmentation. The software provides two types of adaptive segmentation methods. One is the Seeded Region Growing (SRG) first described in [1] and the other is the Globally Optimal Geodesic Active Contours (GOGAC) first described in [2]. These two methods segment a spot by its shape. The spot is adaptive in size and can be of irregular shape.

The method we used in this paper also belongs to the adaptive shape segmentation method. The Active Contour Without Edges (ACWE) method can detect objects' boundary by solving numerical finite differences equations. Experimental results showed that ACWE is better than other adaptive shape methods SRG and GOGAC. It is obvious that ACWE is better than fixed circle and adaptive circle methods. To compare ACWE with the histogram method, we choose spotSegmentation for comparison. The experimental results showed also that ACWE was better.

2. Image analysis methods and basic definitions

There are three steps for microarray image analysis as described in [8]: addressing, segmentation and information extraction. In our research we will not focus on the addressing part since we can get the grid information for the microarray data file from the Stanford website mentioned above. A spot is an area where printed cDNA is located. Segmentation is a partition process used to separate a spot area from a non-spot area. The spot area is called foreground and the non-spot area is called background. We will focus on four types of segmentation methods: fixed circle segmentation, adaptive circle segmentation, adaptive shape segmentation and histogram segmentation. Fixed circle segmentation is an ideal method, it assumes that each spot has the same size and a circular shape. The segmentation algorithm in this case is easy to implement but the real spots may not have the perfect circular shape and same size. Adaptive circle segmentation allows for the diameter of each spot circle to be adjusted. It is better than the fixed circle, but still the spot shape is restricted to be a circle. Histogram segmentation uses the normal distribution of pixels intensity percentiles around and inside each spot to segment the spot from the background. Obviously this method neglects the particular pixels locations. It will not give out the accurate spot intensity but only return the trend. Adaptive shape segmentation is designed to improve the accuracy of the segmentation. This method is better than the fixed and adaptive circle segmentation methods. Watershed, seed region growing and globally optimal geodesic active contours are the three algorithms usually used that fall into the adaptive shape segmentation method class. Watershed segmentation [3] defines an image as a topographic surface and assumes the water enters from the minima and floods the surface. The only visible surface after the flood is called the watershed lines. Watershed segmentation has the weakness of overlaying the original image. The segmentation area of watershed is always larger than that of the original image. Seeded region growing **(SRG)** segment is a method that starts with some seeds (starting points) and then includes the neighboring pixels to check if they have similar intensities. In the affirmative case, the pixels are "joined" together, if not, they will be in different classes. This process will continue until all the pixels have been included in a class containing one of the seeds. The weakness of seeds region growing is that if the seeds were chosen improperly the segmentation result will not be accurate. Globally Optimal Geodesic Active Contours **(GOGAC)** is the new segmentation method which was implemented in [10] Spot **(fall 2007)**. The weakness of this method is that it prefers to produce circles, it cannot prevent overlaps and it is slower than the SRG method. In what follows we will compare also the segmentation results with our implemented method.

The segmentation method we implemented was based on Active Contours Without Edges **(ACWE)** method, which was proposed by Tony F. Chan and Luminita A. Vese in [4]. Chan and Vese (C-V) model is segmenting an image by detecting different objects boundary. The authors assumed an image was formed by two regions within and outside an object. Their model can find out objects within an image without any definition of gradient. The algorithm as described in [4] is as follows:

Algorithm:

1. Initialize ϕ^0 by ϕ_0, $n = 0$.
2. Compute $c_1(\phi^n)$ and $c_2(\phi^n)$ by

$$c_1(\phi^n) = \frac{\int_\Omega \mu_0(x,y)H(\phi(x,y))dxdy}{\int_\Omega H(\phi(x,y))dxdy}$$

and

$$c_2(\phi^n) = \frac{\int_\Omega \mu_0(x,y)(1-H(\phi(x,y)))dxdy}{\int_\Omega (1-H(\phi(x,y)))dxdy}.$$

3. Solve the PDE in ϕ from

$$\frac{\partial \phi}{\partial t} = \delta_\varepsilon(\phi)[\mu div(\frac{\nabla \phi}{|\nabla \phi|}) - v - \lambda_1(u_0 - c_1)^2 + \lambda_2(u_0 - c_2)^2] = 0 \text{ in } (0,\infty)\times\Omega,$$

$$\phi(0,x,y) = \phi_0(x,y) \text{ in } \Omega,$$

$$\frac{\delta_\varepsilon(\phi)}{|\nabla\phi|}\frac{\partial \phi}{\partial \overrightarrow{n}} = 0 \text{ on } \partial\Omega,$$

where $\overrightarrow{n}$ is the exterior normal to the boundary $\partial\Omega$, and $\dfrac{\partial\phi}{\partial\overrightarrow{n}}$ is the normal derivative of ϕ at the boundary.

4. Reinitialize ϕ locally to the signed distance function to the curve (optional).
5. Check whether the solution is stationary. If it is not, then $n = n+1$ and repeat the algorithm.

The C-V model was implemented as in [4] using finite differences equations:

$$\begin{aligned}\frac{\phi_{i,j}^{n+1} - \phi_{i,j}^n}{\triangle t} &= \delta_h(\phi_{i,j}^n)[\frac{\mu}{h^2}\triangle_-^x.(\frac{\triangle_+^x \phi_{i,j}^{n+1}}{\sqrt{(\triangle_+^x\phi_{i,j}^n)^2/(h^2) + (\phi_{i,j+1}^n - \phi_{i,j-1}^n)^2/(2h)^2}}) \\ &+ \frac{\mu}{h^2}\triangle_-^y.(\frac{\triangle_+^y \phi_{i,j}^{n+1}}{\sqrt{(\phi_{i+1,j}^n - \phi_{i-1,j}^n)^2/(2h)^2 + (\triangle_+^y\phi_{i,j}^n)^2/(h^2)}}) \\ &- v - \lambda_1(u_{0,i,j} - c_1(\phi^n))^2 + \lambda_2(u_{0,i,j} - c_2(\phi^n))^2].\end{aligned}$$

The C-V method is the minimization of an energy based segmentation. For example, an image is denoted by u_0 with the boundary denoted by C_0. The image can be divided by two regions: the inside object denoted by u_0^i and the outside object denoted by u_0^o .

The fitting function is defined as follows:

$$F_1(C) + F_2(C) = \int_{inside(C)} |u_0(x,y) - c_1|^2 dxdy + \int_{outside(C)} |u_0(x,y) - c_2|^2 dxdy,$$

where C is the variable curve, c_1, c_2 are the constants depending on C and C_0 is the minimum of the fitting function

$$\inf_C\{F_1(C) + F_2(C)\} \approx 0 \approx F_1(C_0) + F_2(C_0).$$

In the C-V model the fitting function is minimized and some more terms are added like the length of the curve and the area inside the C . The energy function $F(c_1, c_2, C)$ is defined as follows:

$$\begin{aligned} F(c_1, c_2, C) &= \mu \cdot Length(C) + v \cdot Area(inside(C)) + \\ &+ \lambda_1 \int_{inside(C)} |u_0(x, y) - c_1|^2 dxdy \\ &+ \lambda_2 \int_{outside(C)} |u_0(x, y) - c_2|^2 dxdy, \end{aligned}$$

where $\mu \geq 0, v \geq 0, \lambda_1, \lambda_2 \geq 0$ are constant.

The ACWE method minimizes the energy function to get the boundary where $\phi = 0$. The inside part ($\phi > 0$) is the segmentation result needed. It means that the boundary curve has been found and the area inside the boundary is the actual object obtained by the segmentation.

The C-V model has some limitation. For example it cannot detect the texture image. These limitations have no effect on applying the C-V model to cDNA microarray image segmentation. If we apply the ACWE method directly on the whole microarray image it would not give us the correct segmentation. Therefore we made some adjustment for applying ACWE on the microarray image as follows:

1. We used ACWE to segment each spot patch one at a time.
2. We provided the grid file which gives the approximate spot locations.
3. We decreased the iteration numbers and made the computing time shorter by taking into consideration the current segmentation setting.
4. We adjusted the μ value and found smaller spots.

We use C-V method to compute the exact boundary of each spot. We can get the exact location of each spot beforehand by using the grid file from the database. The grid file gives out the location of each spot which will be printed on the microarray during the printing process of the microarray. We use the spot patch which is the location (rectangle or square) of each spot as a sub image. Since the patch outside of every spot is the same, we only need to preset up the initial function and other parameters once for PDE equations. After solving the equations we will get the exact boundary of the individual spot and the intensity value of that spot. To compute the background intensity value, we use the local background. The background area considered in this paper is defined as the area that lies outside the boundary of

the spot and inside the boundary of the spot patch. In the segmentation of cDNA microarray, some parameters are set as follows: $\lambda_1 = \lambda_2 = 1$, $v = 0$, $h = 1$, $\triangle t = 0.1$. The other parameters need adjusting based on the spot size of different microarrays. For example, for cDNA microarray, the initial curve can be chosen inside each spot patch. Smaller μ, ϕ_0 are chosen for spots. Once these parameters are set in the program, there is no need to adjust the parameters during computing, since the spots size for an image are the same based on the grid file.

3. Experimental result

We used real cDNA microarray images from [9] for segmentation. The experiment results showed that ACWE is the most accurate segmentation method out of the five segmentation methods considered.

Figure 1 represents an original 16-bit tagged image file format (TIFF) file.

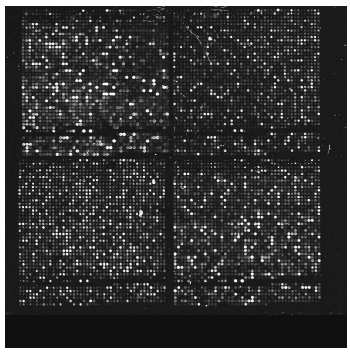

Fig. 1. Original image.

In Figure 2 we present a segmentation result image using the ACWE segmentation method. The red lines around each spot represent the boundary of the spot. The boundary of each spot in Figure 2 using ACWE method gives out almost the actual boundary which can be checked by visual inspection.

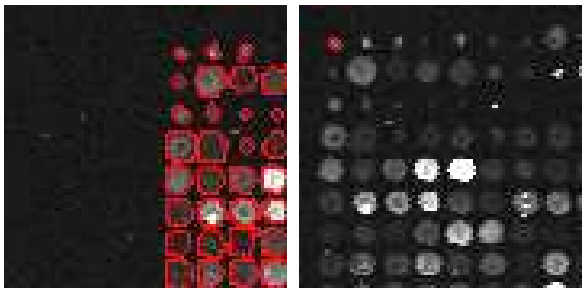

Fig. 2. Left: Image after segmentation using ACWE, right: only spot 1 segmented with ACWE.

Figure 3 presents the segmentation result image obtained by using the GOGAC and SRG segmentation methods. The red lines around each spot is the boundary of the spot.

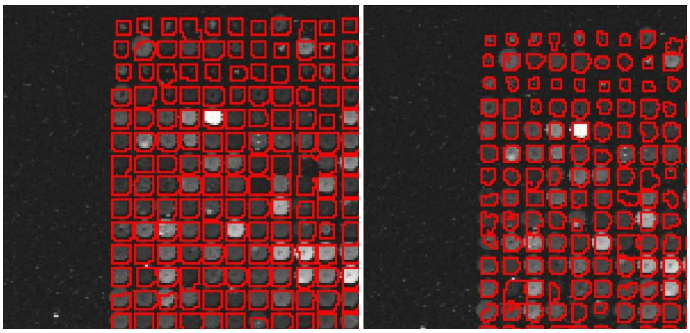

Fig. 3. Segmentation using GOGAC(left) and SRG (right), Spot 1 is at top left corner with red line boundary.

Comparing Figure 2 with Figure 3 we observe that the ACWE method gives a more accurate boundary than the previous two methods mentioned.

In Figure 4 we provide a segmentation image using the spotSegmentation for only one spot (Spot 1). The spotSegmentation is based on histogram segmentation. Comparing Figure 2 and Figure 4, we visually observe that the ACWE method gives out more accurate boundary than the spotSegmentation method . These two methods were segmenting the same spot from the same original image. The same spot (Spot 1) can also be found in Figure 3 at the top left corner.

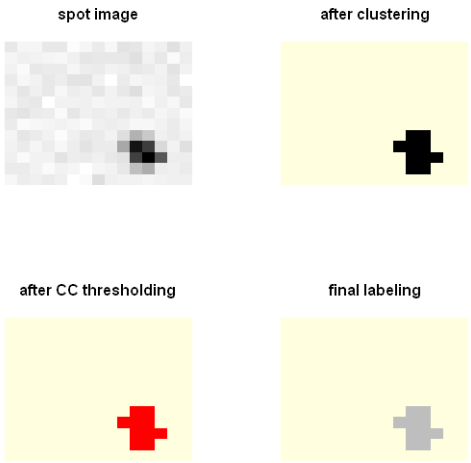

Fig. 4. Segmentation using spotSegmentation for Spot 1.

Figure 5 shows the pixel intensities for Spot 1. The 10 columns by 10 rows square is the patch for Spot 1. After segmentation using ACWE the area with 5 pixels

(yellow part) is the exact Spot 1. The red figures are the boundary which separates the Spot 1 with the background.

Based on Figure 5 the mean intensity value of Spot 1 was computed as $(2576 + 1648 + 1640 + 2456 + 1896)/5 = 2043$. The actual mean intensity value of Spot 1 was computed by different methods and the result is as follows:

Spot 1	ACWE	SRG	GOGAC	Fixed circle	spotSegmentation
mean intensity	2043	1308	693	414	1279

The result showed that other segmentation methods counted more pixels to the Spot1 and thus got the less mean intensity value. Only ACWE method can segment the Spot 1 correctly.

296	336	280	272	368	200	272	256	256	288
336	232	280	248	272	216	344	248	344	360
248	256	288	312	240	304	272	296	264	248
296	304	264	312	304	224	272	344	216	336
336	320	296	336	720	464	296	336	272	248
336	320	336	520	2576	1648	384	280	344	304
288	296	328	368	1640	2456	1896	272	328	296
272	288	280	336	472	400	296	240	312	272
256	392	264	248	336	272	248	288	288	320
304	280	240	288	216	272	336	296	184	288

Fig. 5. Segmentation by ACWE of Spot 1: yellow is the spot area, red is the boundary.

In Figure 6, the 3D visualization picture of figure 5 was presented. The intensity value of each pixel was used as Z-axis. The 5 pixels with extremely high intensities were partitioned as the spot foreground.

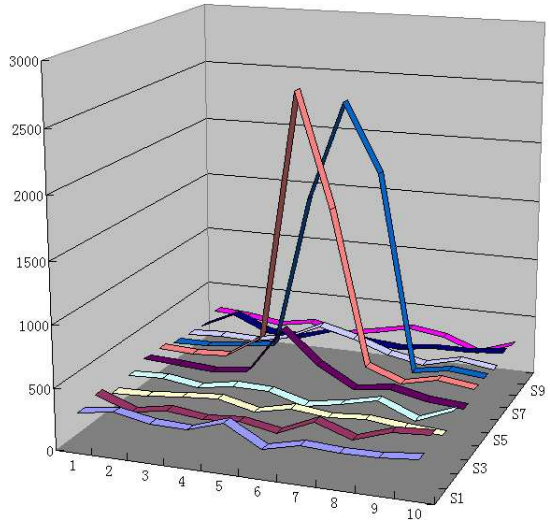

Fig. 6. 3D graphic for spot patch of spot 1 with intensity value. Z-axis is the intensity value. 5 pixels with extreme high intensity are partition to the same spot foreground.

In what follows we will perform linear regression analysis in order to investigate the relationships between the ACWE method and the SRC, GOGAC and Fixed circle methods. The same microarray image was segmented using these different methods, the spots intensities were calculated using each of the methods. Then the linear model was determined for each case. Figure 7 presents the linear regression line and the model equation that explains the relation between the ACWE and SRG methods. We observe that $R^2 = 0.9714$.

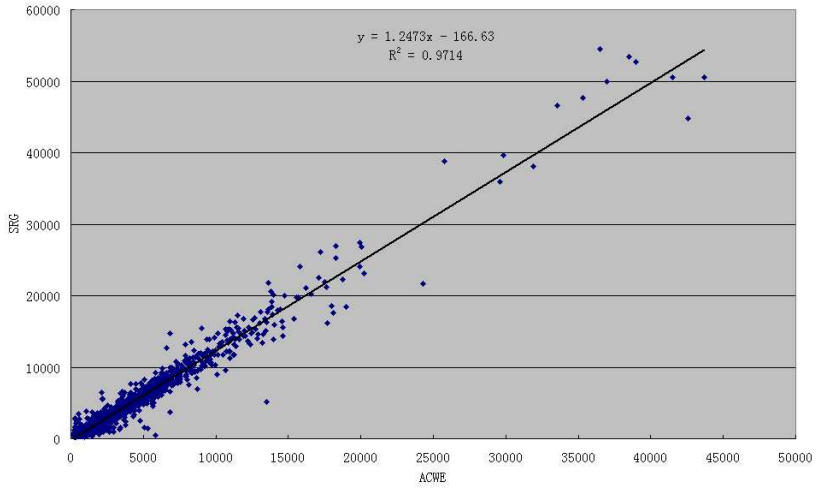

Fig. 7. The linear regression between SRG and ACWE methods.

Figure 8 presents the linear regression line and the model equation that explains the relation between the ACWE and GOGAC methods. We observe that $R^2 = 0.9662$.

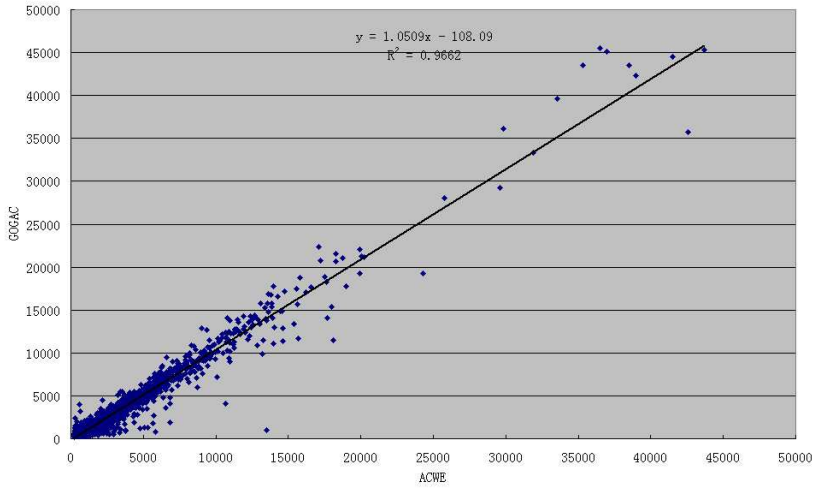

Fig. 8. The linear regression between GOGAC and ACWE methods.

Similarly Figure 9 presents the linear regression line and the model equation that explains the relation between the ACWE and Fixed circle methods. We observe that $R^2 = 0.6494$.

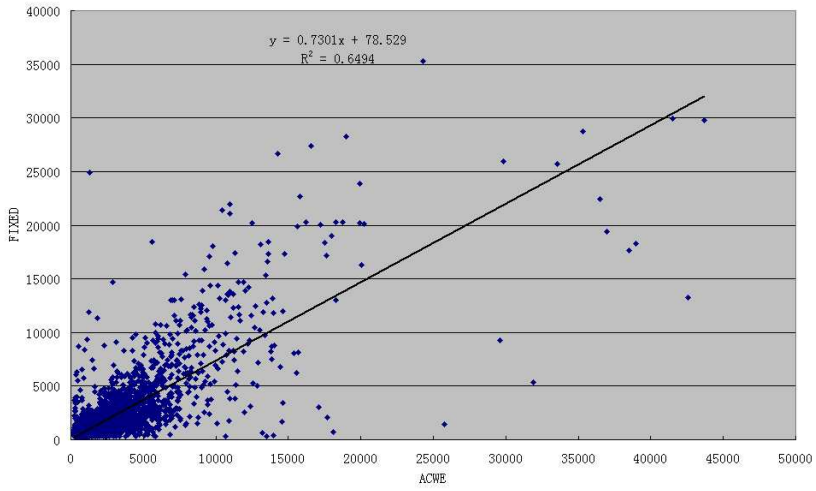

Fig. 9. The linear regression between FIXED circle and ACWE methods.

Therefore, observing the regression lines in Figures 7 - 9 we conclude that ACWE was highly correlated with SRG and GOGAC and least correlated with the fixed circle methods. The ACWE method is the most accurate in determining the boundary of the spots.

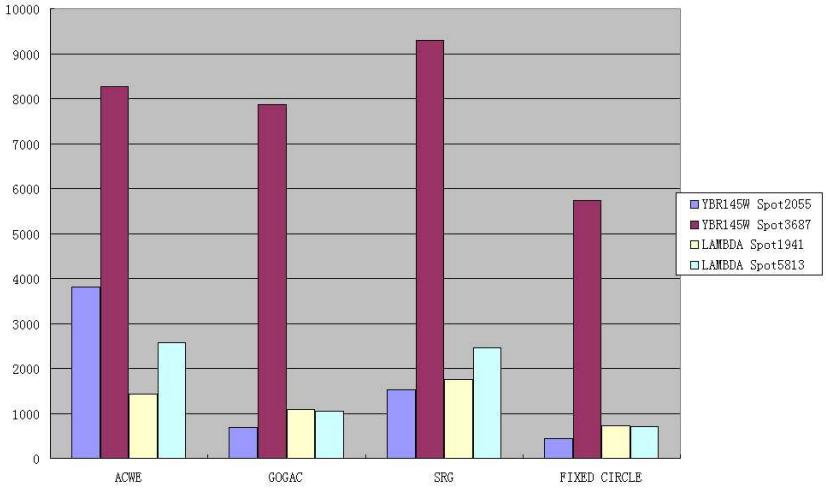

Fig. 10. LAMBDA is a control spot and YBR145W is a gene spot. The trend is the result of intensity of the spots using different methods.

Figure 10 presents the comparison between control spots and spots with same gene. LAMBDA was a control spot and YBR145W was a gene spot (with gene named "ADH5"). For the two gene spots (Spot 2055 and Spot 3687), ACWE had smaller difference between them. For the two control spots (Spot 1941 and Spot 5813), the ACWE method showed bigger difference between the two controls.

In Figure 11 we present the boxplot of log ratio on spots named "LAMBDA". The inter-quantile range (IQR) presented method ACWE was better than the ones provided by the SRG and GOGAC methods, since it showed a smaller range which meant less gene expression differences for the control spot.

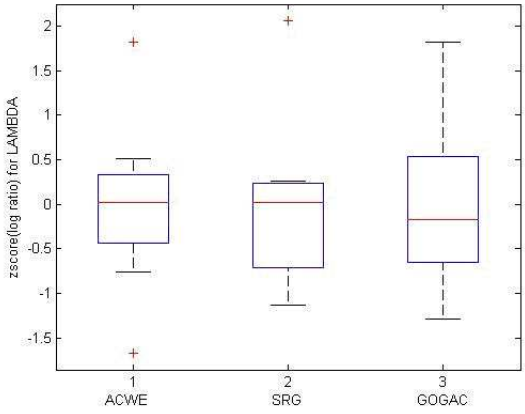

Fig. 11. Boxplot of z-score normalization of log ratio using different methods.

According to [7], Figure 12 given in he following shows the gene clusters with cell cycle-regulated and the histone (a key protein component) cluster under the alpha factor experiment. Figure 12 was presented as an array with 9 rows and 18 columns. Each row represents a gene and each column represents a microarray image. Histone genes showed periodical regulation. There are 9 genes in Figure 12. Only eight genes were used in the experiment data set which were 'HTB2, HTA2, HHF1, HHF2, HHT2, HHB1, HHT1, HTA1'. Totally 18 microarray images were used in the alpha factor experiment. Each image was taken every 7 minutes in a time series. Figure 14 showed a clear cell cycle in Alpha Factor section under cluster histone. It showed 'Green Red Green Red' cycle. Approximately, at minute 0, 7 and 14, it showed green. At minute 28, 35 and 42, it showed red. At minute 63 and 70, it showed green again. At minute 84, 91 and 98, it showed red again. Red showed the DNA expression was increased. Black showed the DNA expression was stable. Green represented the DNA expression was decreased.

We stress that according to [7] the data presented in the following figure was built manually by the researchers (counting the intensities of the spots manually). We therefore will consider this information as control data (as it is curated) and will use it to compare the different segmentation methods.

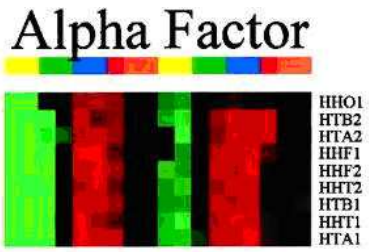

Fig. 12. Histone genes under yeast alpha factor experiment.

In the following we will focus on minute 70 of the experiment (when according to [7] the log ratio values should be negative) green in Figure 12.

Figure 13 shows the 'Green Red Green Red' cycle which was the same as in Figure 14. The ratio R_g is equal to $\frac{Y_g}{X_g}$. This ratio represents the DNA change (DNA expression difference).X_g denotes the gth spot pixel intensity of Cy3 channel (Green). Y_g denotes the g^{th} spot pixel intensity of Cy5 channel (Red). Logarithms of this ratio is $log_2 R_g$. Using logarithmic transformation reduces the skewness of the distribution and improves the variance estimation. Log ratio of intensities from Red and Green channel was computed to represent histone genes expression in alpha factor using the ACWE method.

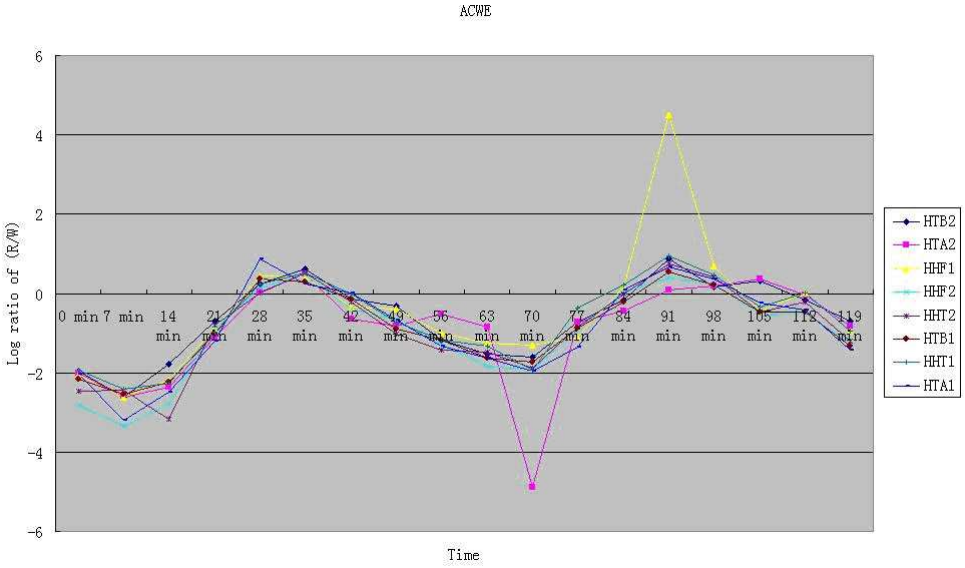

Fig. 13. Log ratio (R/G) of histone genes in alpha factor using ACWE method.

In Figure 14 log ratio of intensities from Red and Green channel was computed to represent histone genes expression in alpha factor using the SRG method. At minute 70, it showed red. This is different from Figure 12.

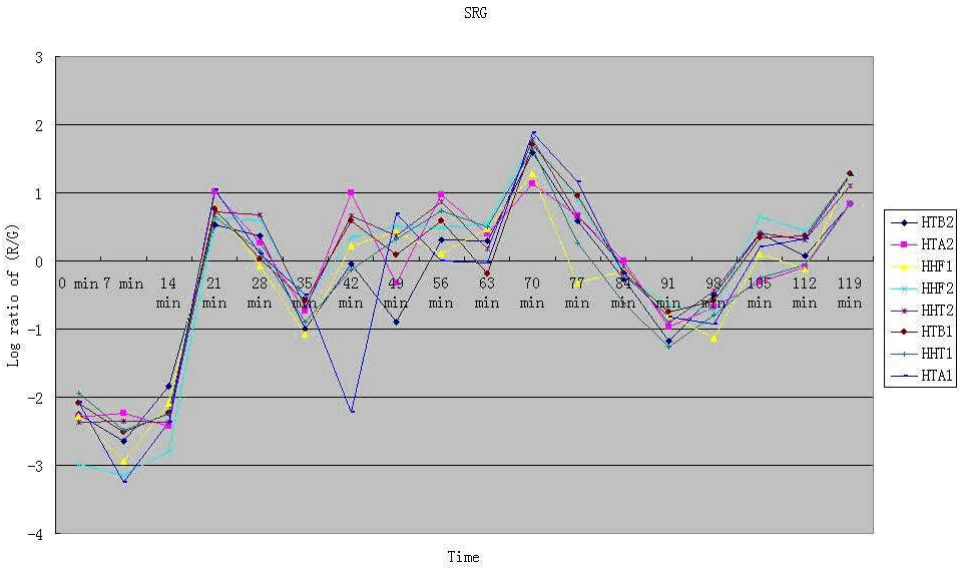

Fig. 14. Log ratio (R/G) of histone genes in alpha factor using SRG method.

In Figure 15 the log ratio of intensities from Red and Green channel was computed to represent histone genes expression in alpha factor using the GOGAC method. At minute 70, it showed red. This is different from Figure 12.

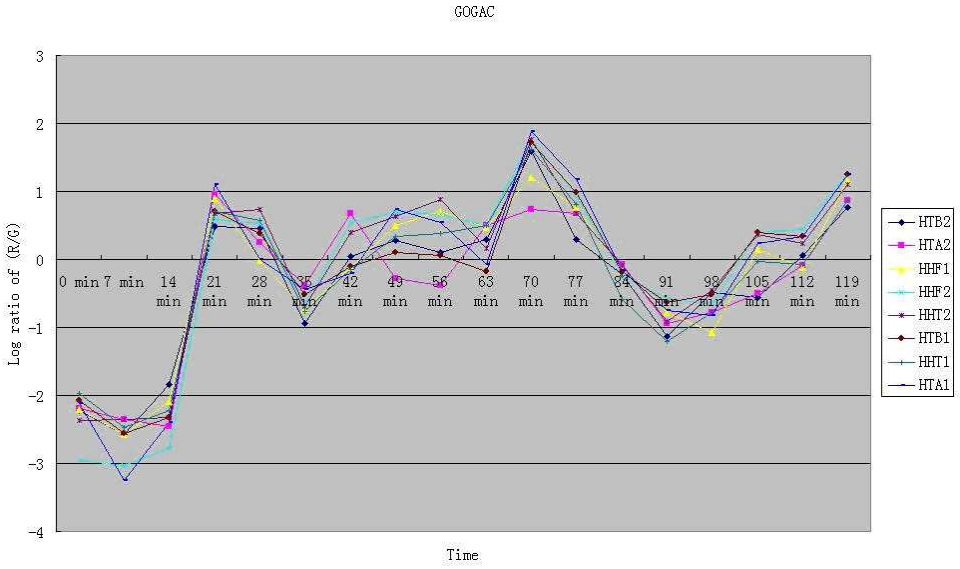

Fig. 15. Log ratio (R/G) of histone genes in alpha factor using GOGAC method.

Therefore, we can conclude that ACWE is better than SRG and GOGAC since it matched the exact biological cell cycle.

4. Conclusion

Active Contour Without Edges ACWE segmentation method is more accurate in extracting the spots foreground intensities than the other segmentation methods discussed above. The log ratio based on the ACWE segmentation can provide more accurate gene expression difference levels than the other segmentation methods. The accurate intensities data provided are much more helpful in the cluster analysis, function prediction of data mining for future analysis. These accurate intensities data are much more helpful in the cluster analysis, function prediction for future analysis.

We have shown that the ACWE method is outperforming the current segmentation methods used today. The big drawback of the method proposed in the current paper is its requirements with respect of time: in our processing we showed a time difference of about 80 fold between ACWE and the other methods. This means that if the processing takes now minutes for an array, it could take of the order of hours in the case of ACWE. This should not be a deterrent towards ACWe because the actual biological experiments (preparation of the cells, preparation of the DNA chip, etc.) takes usually of the order of days, thus it does not make any sense to hurry-up in the end and obtain the results fast but not the most accurate. With the advent of higher resolution cameras we anticipate that the increase in resolution will show an even wider gap between ACWE and other methods, with ACWE becoming even more accurate. If at the moment we estimate that around 3% of the values computed in a DNA chip have different values between ACWE and GOGAC, a higher resolution picture should increase this percentage. Considering that out of the total of tens of thousands of spots a successful experiment identifies roughly tens of genes, a 3% change in the number of values can prove to have dramatic changes in the results and conclusions of the work.

Up until now the DNA arrays have been considered as qualitative tools (due to the problems related to sensitivity and reliability in the value association with the genes), we consider that our approach could be a first step into the direction of DNA arrays that are quantitative. Of course, the technology needs to be bettered also at the hardware/experimental level, but at the image processing level the ACWE method should provide excellent results once the resolution of the pictures is increased.

5. Future work

Parallel computing may be implemented in the ACWE to improve the computing time. We can also apply ACWE method to Affymetrix Genechip. By segmenting the Affymetrix GeneChip .DAT image files, the gene cell intensity values can be obtained. We want to show that ACWE can also provide more accurate segmentation result of gene cell intensity than the method Affymetrix applied. Each Affymetrix GeneChip probe cell is constructed with n*n pixels. When Affymetrix software segmenting the spot intensity, it uses the inner (n-2)*(n-2) pixels. The outer boundary of 4*(n-1) pixels are excluded. The average intensity of the probe cell (spot) is computed by using the 75 percentile of the (n-2)*(n-2) pixels. It doesn't care about the real shape

of the probe cell. ACWE can provide the real shape of each probe cell and give more accurate intensity value for each probe cell. We will do more experiments based on Affymetrix image files to show ACWE is better.

Acknowledgements. Work supported in part by NSF Grant CCF-0523572, INBRE Program of the NCRR (a division of NIH), support from CNCSIS grants RP-13/2007 RP-5/Jan. 2008, support from CNMP grant 11-56 /2007, support from Spanish Ministry of Science and Education (MEC) under project TIN2006-15595, and support from the Comunidad de Madrid (grant No. CCG07-UPM/TIC-0386 to the LIA research group).

References

[1] ADAMS R., BISCHOF L., *Seeded region growing*, IEEE Transactions on Pattern Analysis and Machine Intelligence, **16**, pp. 641–647, 1994.

[2] APPLETON B., TALBOT H., *Globally optimal Geodesic Active Contours*, Journal of Mathematical Imaging and Vision, **23**, pp. 67-86, 2005.

[3] BEUCHER S., MEYER F., *The morphological approach to segmentation: the watershed transformation*, in *Mathematical Morphology in Image Processing*, vol. **34** of *Optical Engineering*, chapter 12, Marcel Decker, New York, pp. 433–481, 1993.

[4] CHAN T. F., VESE L. A., *Active Contours Without Edges*, IEEE Transactions On Image Processing, Volume **10**, Issue 2, Feb 2001, pp. 266–277.

[5] CHEN Y., DOUGHERTY E. R., BITTNER M. L., *Ratio-based decisions and the quantitative analysis of cDNA microarray images*, J. Biomedical Optics, Joseph R. Lakowicz; Ed. 2(04), pp. 364–374.

[6] SIMON R. M., KORN E. L., MCSHANE L. M., RADMACHER M. D., WRIGHT G. W., ZHAO Y., *Design and analysis of DNA microarray investigations*, Springer 2003, ISBN 0-387-00135-2.

[7] SPELLMAN P. T., SHERLOCK G. A., ZHANG M. Q., IYER V. R., ANDERS K., EISEN M. B., BROWN P. O., BOTSTEIN D., FUTCHER B., *Comprehensive Identification of Cell Cycle-regulated Genes of the Yeast Saccharomyces cerevisiae by Microarray Hybridization*, Molecular Biology of the Cell, Volume **9**, Issue 12, pp. 3273–3297, December 1998.

[8] YANG Y. H., BUCKLEY M. J., DUDOIT S., SPEED T. P., *Comparison of methods for image analysis on cDNA microarray data*, Journal of Computational & Graphical Statistics, Volume **11**, Number 1, 2002 , pp. 108–136(29).

[9] `http://genome-www.stanford.edu/cellcycle/data/rawdata/individual.html`

[10] `http://www.hca-vision.com/Spot_Documentation/Spot.pdf`